Eur. Phys. J. Plus (2015) **130**: 187
DOI 10.1140/epjp/i2015-15187-0

THE EUROPEAN PHYSICAL JOURNAL PLUS

Regular Article

Looking at the sub-TeV sky with cosmic muons detected in the EEE MRPC telescopes

M. Abbrescia[1,2], C. Avanzini[1,3], L. Baldini[1,3], R. Baldini Ferroli[1,4], G. Batignani[1,3], G. Bencivenni[4], E. Bossini[1,5], E. Bressan[1,6], A. Chiavassa[7], C. Cicalo[1,8], L. Cifarelli[1,6], E. Coccia[9], A. Corvaglia[1,10], D. De Gruttola[1,11], S. De Pasquale[1,11], A. Di Giovanni[12], M. D'Incecco[12], M. Dreucci[4], F.L. Fabbri[4], E. Fattibene[13], A. Ferraro[13], R. Forster[14,15], V. Frolov[16], P. Galeotti[1,7], M. Garbini[1,6], G. Gemme[16], I. Gnesi[1,7], S. Grazzi[1,17], C. Gustavino[12], D. Hatzifotiadou[1,6,15], P. La Rocca[1,18], A. Maggiora[7], G. Maron[13], M.N. Mazziotta[19], S. Miozzi[1,4,9], F. Nozzoli[20], M. Panareo[1,10], M.P. Panetta[1,10], R. Paoletti[1,5], L. Perasso[1,17], F. Pilo[1,3], G. Piragino[7], F. Riggi[1,18], G.C. Righini[1], A. Rodriguez Rodriguez[14,15], G. Sartorelli[1,6], E. Scapparone[6], M. Schioppa[1,21], A. Scribano[1,3], M. Selvi[6], S. Serci[7], E. Siddi[8], S. Squarcia[17], M. Taiuti[17], G. Terreni[3], M.C. Vistoli[13], L. Votano[12], M.C.S. Williams[5,15], S. Zani[13], A. Zichichi[1,6,15], and R. Zuyeuski[14,15]

[1] Museo Storico della Fisica e Centro Studi e Ricerche Enrico Fermi, Roma, Italy
[2] INFN and Dipartimento Interateneo di Fisica, Università di Bari, Bari, Italy
[3] INFN and Dipartimento di Fisica, Università di Pisa, Pisa, Italy
[4] INFN, Laboratori Nazionali di Frascati, Frascati (RM), Italy
[5] INFN Gruppo Collegato di Siena and Dipartimento di Fisica, Università di Siena, Siena, Italy
[6] INFN and Dipartimento di Fisica e Astronomia, Università di Bologna, Bologna, Italy
[7] INFN and Dipartimento di Fisica, Università di Torino, Torino, Italy
[8] INFN and Dipartimento di Fisica, Università di Cagliari, Cagliari, Italy
[9] INFN and Dipartimento di Fisica, Università di Roma Tor Vergata, Roma, Italy
[10] INFN and Dipartimento di Matematica e Fisica, Università del Salento, Lecce, Italy
[11] INFN and Dipartimento di Fisica, Università di Salerno, Salerno, Italy
[12] INFN, Laboratori Nazionali del Gran Sasso, Assergi (AQ), Italy
[13] INFN CNAF, Bologna, Italy
[14] ICSC World Laboratory, Geneva, Switzerland
[15] CERN, Geneva, Switzerland
[16] JINR, Joint Institute for Nuclear Research, Dubna, Russia
[17] INFN and Dipartimento di Fisica, Università di Genova, Genova, Italy
[18] INFN and Dipartimento di Fisica e Astronomia, Università di Catania, Catania, Italy
[19] INFN, Sezione di Bari, Bari, Italy
[20] INFN and ASI Science Data Center, Roma, Italy
[21] INFN and Dipartimento di Fisica, Università della Calabria, Cosenza, Italy

Received: 22 July 2015 / Revised: 31 August 2015
Published online: 25 September 2015 –

Abstract. Distributions of secondary cosmic muons were measured by the Multigap Resistive Plate Chambers (MRPC) telescopes of the Extreme Energy Events (EEE) Project, spanning a large angular and temporal acceptance through its sparse sites, to test the possibility to search for any anomaly over long runs. After correcting for the time exposure and geometrical acceptance of the telescopes, data were transformed into equatorial coordinates, and equatorial sky maps were obtained from different sites on a preliminary dataset of 110 M events in the energy range at sub-TeV scale.

1 Introduction

It is known that cosmic rays below the knee (3×10^{15} eV) are of galactic origin, since the transition between galactic and extragalactic origin lies around energies of 10^{18}–10^{19} eV. Galactic cosmic rays are expected to be nearly isotropic, due to their interaction with the galactic magnetic field over the long path to the Earth. Observation of cosmic rays at energies sensibly smaller than 10^{15} eV is a useful tool to inspect the magnetic field structure in the interstellar

environment close to our Solar System. In this energy range small anisotropies may be induced by large scale as well as local magnetic field features, which may cause deviations from the isotropic diffusion model. At very low primary energies, of the order of 1 TeV, even sizeable effects from the eliosphere may be expected on the cosmic ray distributions.

The so-called Compton-Getting effect, introduced in 1935 [1], predicts a dipole component in the cosmic ray anisotropy, due to the motion of the observer with respect to an isotropic cosmic ray plasma rest frame. For instance the anisotropy arising from the Earth motion around the Sun is predicted to be of the order of 10^{-4} and has been observed [2,3].

Over the last few years, detection of primary cosmics in the energy range from several tens of GeV to PeV from various experiments [4–7] has demonstrated that small but measurable anisotropies in the arrival distribution of cosmics may be evidenced. Observed anisotropies are very small, at the level of 10^{-5}–10^{-3}, hence they have required a huge amount of data collected for several years. As an example, the IceCube Collaboration [4] collects a number of muons of the order of 10^{10}–10^{11} per year, allowing for studies of variations in the arrival map distribution down to 10^{-5}. At TeV energies, anisotropies of the order of 10^{-3}, with an excess (tail-in region) around 75° Right Ascension, and a deficit (loss-cone region) around 200° Right Ascension have been observed [8].

Such measurements are based on the assumption that the direction of secondary muons mirrors, within a few degrees, that of the primary particle. If the search for point sources is not of special concern in this low-energy regime, the distribution over an extended area in equatorial coordinates (Right Ascension, Declination) allows not only for the observation of the existence of anisotropies but also for a quantitative investigation of its shape provided that the needed statistics is collected. The anisotropy may vary with the energy of the particles, even if the topological structures observed so far in the equatorial coordinate distribution of events do not change up to about 100 TeV, whereas some evidence of changes in these strctures are only observed above 100 TeV [4].

In the case of IceCube, an energy cut around 20 TeV was imposed by the detector configuration and by the amount of ice traversed by the particles, whereas larger energies, above 100 TeV, were probed by the surface array IceTop detector, which collects the low-energy electromagnetic and muonic components of the shower.

Looking at very low primary energies, such as those probed by the inclusive detection of secondary cosmic muons at the sea level, may give the possibility to explore the sky in a restricted energy region, where the influence of local eliospheric and terrestrial phenomena could produce non-uniformity over space and time. A large statistics is in any case required to produce significant maps where excess or deficit regions might be evidenced. The Extreme Energy Events (EEE) network [9], which employs several Multigap Resistive Plate Chambers (MRPC) telescopes, able to detect cosmic muons and reconstruct their arrival direction, is in principle a good candidate to collect enough data to explore the sky at sub-TeV energies. Continuous running of the EEE telescopes allows for a search of variations in the sky map along different periods of the year and over different sites.

In this paper we report preliminary results of an investigation aimed at evaluating the experimental conditions under which the observation of the cosmic ray sky map for primary energies below the TeV may be carried out. Geometrical acceptances and time exposure of the EEE telescopes were evaluated. CORSIKA simulations of low-energy extensive air showers were caried out, to quantify the spread of secondary muons around the primary axis. The effect of the multiple scattering of muons due to the structure of the buildings where the EEE telescopes are located was also studied. Both effects help to understand the optimal size of the angular grid to be used for the sky map. Data from a first set of about 110 M events, collected by different EEE telescopes, were then used to produce sky maps in equatorial coordinates and check for isotropy/anisotropy effects along the map.

2 The experimental setup and running conditions

2.1 The EEE Project

The EEE Project is a joint educational and scientific initiative by Centro Fermi (Museo Storico della Fisica e Centro Studi e Ricerche Enrico Fermi) [9], in collaboration with INFN (National Institute for Nuclear Physics), CERN and MIUR (the Italian Ministry of Education, University and Research). The Project has built and installed an array of cosmic ray detectors, distributed in several sites, spanning all the Italian territory, over an area larger than 3×10^5 km^2.

The research goals of the Project include the study of the properties of the local muon flux and its dependence on planetary and solar environment, the detection of high-energy extensive air showers created in the Earth atmosphere by time and orientation correlations between several telescopes, and the search for possible long-range correlations between far telescopes.

A powerful impact on education is also envisaged by the EEE Project, which is strongly contributing to introduce a large number of school teachers and students to the problems and results of particle and astroparticle physics.

Several results from the EEE Project have already been reported [10–16]. At present, more than 40 telescopes are actively taking data since several years, and after a Pilot Run at the end of 2014, which resulted in a number of

collected events of the order of 10^9, the RUN1 was successfully organized, with about 40 telescopes participating in the data taking for a two months period (March–April 2015) and an overall number of collected events around 4×10^9.

2.2 The MRPC telescopes

The detection technique employed by the EEE telescopes, based on Multigap Resistive Plate Chambers, is able to provide the orientation of each incoming muon, with a high efficiency and angular resolution.

Each EEE telescope is composed of three MRPCs [14,15] ($0.82 \times 1.58\,\mathrm{m}^2$ active area), built at CERN by high-school teams under the supervision of researchers and technicians. Typical distances between the chambers are 40–80 cm in the different installations. Each chamber has six gas gaps obtained by means of a sandwich of glass plates spaced by 300 μm. A continuous gas flow with a mixture of $C_2H_2F_4$ (98%) and SF_6 (2%) in the chambers is provided by a gas mixing station. The high voltage applied to the outer glasses, up to ± 10 kV, generates a uniform electric field between the glass electrodes.

Each MRPC is equipped with 24 copper strips (160 cm long, with a pitch of 3.2 cm) as signal pick-up electrodes, on both anode and cathode. The overall thickness of the sensitive part of the MRPC chamber is about 1 cm. A six-fold coincidence of the left and right front-end cards of the three MRPCs generates the data acquisition trigger. To tag each event, for the purpose of combining the information collected by different telescopes, the absolute time of each event is also recorded with a GPS unit. This was a VME Hytec module in the first EEE telescopes, while more recent installations make use of a Spectracom GPS unit installed in a slot of the acquisition PC. Comparative tests between the two units were carried out at the beginning to ensure proper synchronization between different sites.

The particle impact point on each MRPC plane is reconstructed by the hit strips —in one direction— and by the time difference in the arrival of signals at each strip end in the other direction, with a spatial resolution of about 0.7 cm for both coordinates. Adjacent hits contribute to define a cluster, by the average of their X- and Y-positions.

A tracking procedure is then applied to the set of cluster points reconstructed from the recorded hits in the three chambers, removing possible non-aligned points by a cut on the quality of the fit, based on the residuals d_1, d_2 and d_3 between the fitted track and the cluster points in each chamber ($(d_1^2 + d_2^2 + d_3^2)^{1/2} < 10$ cm), and choosing the set of aligned clusters with the smallest value in case of multiple clusters. Additional cuts were imposed in the present analysis on the ratio between the track length l, as determined by the reconstructed hits in the three chambers, and the time-of-flight tof between the top and bottom chambers ($l/tof > 20$ cm/ns).

3 Analysis methods

3.1 Transformation of EEE data to equatorial coordinates

The basic way to extract the orientation of a muon track by measurements with one of the EEE telescopes is to employ the local altoazimuthal (also called horizontal) coordinate system. The orientation of a muon track, as derived from a fit performed on the hits detected on the three MRPC chambers, is defined by the values of the azimuthal angle φ (which is usually referred to the magnetic North direction) and by the polar angle ϑ, measured starting from the vertical direction ($\vartheta = 0$), or by the altitude $a = (90 - \vartheta)$.

During installation, MRPC chambers were placed horizontally, by the use of a level, and aligned each other along the X- and Y-positions to within 1 mm. The orientation of each telescope was achieved by a combination of several methods, including the use of a compass placed far away from metal structures and detailed maps of the local area where the building is located.

Such coordinate system is very easy to implement and use, and at a first approximation also allows one to correlate information from two close telescopes. Imposing that the time correlated tracks impinging on two telescopes have similar directions if they come from a single extensive air shower may be simply done evaluating the relative angle ϑ_{12} between the directions (ϑ_1, φ_1), (ϑ_2, φ_2) of the two tracks, and choosing an upper cut (for instance $\vartheta_{12} \leq 10^\circ$). Although this is not strictly correct, due to the Earth curvature, for telescopes which are not so far away, it represents a very good approximation. For instance, muon tracks detected both as vertical in two telescopes located in the same metropolitan area (about 3 km distance) have a relative angle smaller than 0.03°. In case of telescopes located in close towns (30–50 km) this effect amounts to about 0.4°, reaching about 10° for telescopes located very far away (1000 km apart).

More important however is the fact that the use of the horizontal reference system implies that the coordinates of a sky object change with time. For instance, two muon tracks —seen as vertical by the same telescope but at different times— clearly originate from a different region of the sky.

To define the position of any astronomical object, one needs to have a reference frame or coordinate system, in order to unambiguously identify the position of the object by two numerical quantities. While the horizontal system makes use of the plane of the observer's horizon to define the azimuth and altitude of the celestial object, other

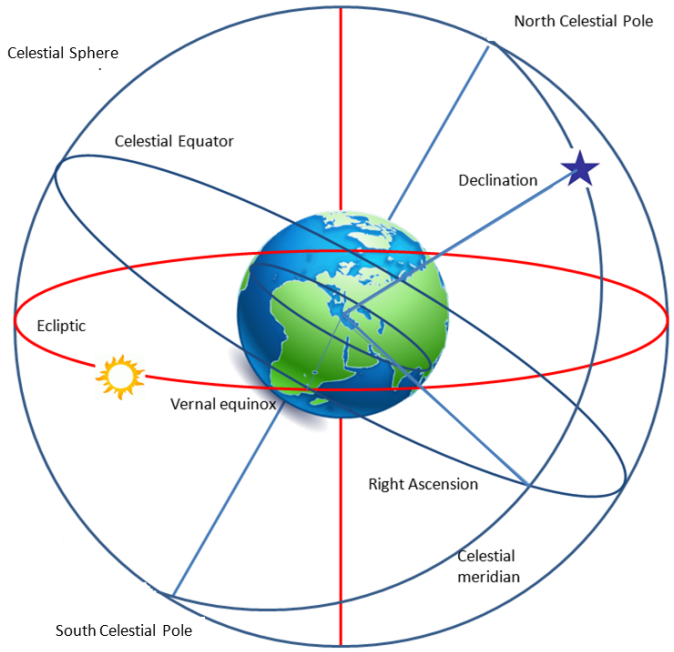

Fig. 1. Schematic view of the equatorial coordinate system.

coordinate systems are largely employed in astronomy. The equatorial coordinate system makes use of the plane of the Earth's equator, extending such plane to cut the celestial sphere. The two coordinates needed in such a system are called the Right Ascension (RA) and the Declination (Dec). The Declination is measured in degrees, positive north of the equator, negative south of it. The Right Ascension may be measured in hours (0 to 24) or in degrees (0 to 360°, or −180° to +180°), and the origin is usually related to a fixed direction in the sky, namely the first point of Aries (vernal equinox), along the line of the intersection of the plane of the Earth's equator with that of the Earth's orbit around the Sun (fig. 1).

This is the common system employed by astronomers to define the position of star objects in the near Universe, for instance the location of individual stars, since such coordinates do not depend on time and have a unique meaning for all observers located in different regions of the Earth. This is then the most convenient system to study the properties of the astronomical environment around the Solar System.

Other coordinate systems exist, which are more convenient when investigating specific aspects of the sky: the ecliptic system, making use of the plane of the Earth's orbit around the Sun, is more convenient for the study of objects belonging to the Solar System while the galactic system, where the reference plane is the plane of our Galaxy and the important direction is that connecting our Sun to the center of the Galaxy, allows for an easy location of stars with respect to the Milky Way.

To move from one reference system to another by the use of appropriate variable transformation requires to know the location of the site on Earth, and the observation time for each event. In our case we need to transform from the horizontal to the equatorial reference system.

Given the orientation of a muon track (altitude a and azimuth φ), its declination δ and hour angle H are given by [17]

$$\sin\delta = \sin a \sin\varphi + \cos a \cos\varphi_L \cos\varphi,$$
$$\cos H = \frac{\sin a - \sin\varphi_L \sin\delta}{\cos\varphi_L \cos\delta},$$

where φ_L is the observer's geographical latitude.

The hour angle H and the Right Ascension RA are related by the formula

$$H = LST - RA$$

where LST is the local sidereal time, which depends in turn on the GPS time associated to the detected event.

A ROOT C^{++} macro, implementing the above mentioned formulas, was employed to read individual events from the data files and calculate the corresponding equatorial coordinates (RA, Dec) on an event-by-event basis. Two-dimensional (RA, Dec) histograms were produced for each day of data taking, both for real events and for fake events, according to the *scrambling* procedure, as described in sect. 3.4.

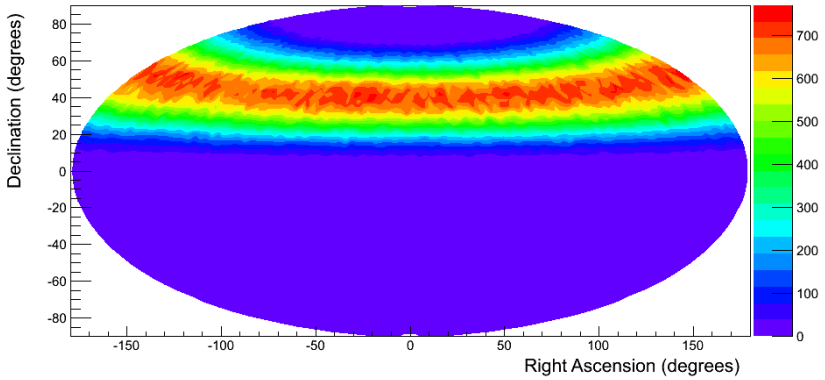

Fig. 2. Aitoff projection of the sky map for one of the EEE telescopes (CATA-01), located around 37° Lat. North, 15° Long. East (see table 1).

The fraction of sky covered by a particular cosmic ray detector depends on its geographical location and on the geometrical acceptance of the detector. Since all the telescopes of the EEE network are presently located in Italy or very close to it (CERN, Geneva), hence along geographical latitudes between 37° and 46° North, they mostly cover that part of the sky between the equator and about 70° in Declination. The coverage in Declination also depends on the largest polar angle with respect to the vertical visible by the telescope, that for most of the telescopes is around 40°. As an example, fig. 2 shows the equatorial map (in Aitoff projection) describing the sky coverage of a telescope situated at about 37° Lat. North, in a whole day (24 hours) of data taking. With an approximate rate of 18 Hz, about 1.5 M events are collected and shown in this figure. The vertical scale, given by the color palette, reports the number of events in each angular bin ($3° \times 3°$).

3.2 Muon orientation with respect to primary shower axis

It is well known that most of the secondary particles produced in the development of an extensive air shower in the Earth atmosphere are concentrated along the direction of the primary particle producing the shower. This near parallelism around the primary axis is the basis for a rough reconstruction of the distribution of the incoming direction of the primary by a single muon detector. The average relative angle of the secondary particles with respect to primary depends however on several factors, namely the species of secondary products being considered, their energy as well as the energy of the primary.

To quantify such aspects in our case, we carried out quantitative CORSIKA [18] (Version 7.4) calculations of extensive air showers initiated by primary protons of various energies, arriving with an isotropic random distribution of their original orientations, between the vertical and 60°. Particles were followed down to the sea level, with only a very small cut on their energy (50 MeV). Proton energies between 10^9 and 10^{17} eV were considered. The number of simulated showers was of the order of 4×10^4 for low-energy primaries, and correspondingly lower for the more energetic showers, in the order of a few hundred. Taking into account the number of muons in the shower, which roughly scales as $E_{primary}^{0.85}$, and the primary flux $\mathrm{d}N_{primary}/\mathrm{d}E = E^{-\gamma}$, with $\gamma = 2.7$ below the knee, the relative probability that each detected muon originates from a particular energy of the primary may be evaluated. As is seen from fig. 3, most of the muons detected at the sea level come from extensive air showers in the range 10^{10}–10^{12} eV.

Secondary muons were selected in the list of produced particles, and for each particle the relative angle with respect to the primary axis was considered (fig. 4). The blue dots report the values obtained taking into consideration all secondary muons. It is expected that muons of higher energy are more concentrated around the primary axis. A cut on the muon energy at 1 and 10 GeV has been applied to filter the data, and the results are shown with green triangles (for those muons of energy higher than 1 GeV) and with red squares (for the muons with energy higher than 10 GeV).

As shown in the plot, at low primary energy, of the order of 10^{11} eV, the average value of the relative angle is about 5°, decreasing to about 4° for more energetic showers. Due to some shielding around most of the EEE telescopes, some muon absorption is always present. As an example, a few concrete layers are able to absorb muons of several hundred MeV. A cut at 1 GeV results in slightly smaller values of the average relative angle (about 3°). Due to the abundance of primary cosmics (as plotted in fig. 3), it may be inferred that for low-energy primaries and low values of the secondary muon energy, within a relative angle of the order of a few degrees, the direction of the incoming muon mirrors that of the original proton direction.

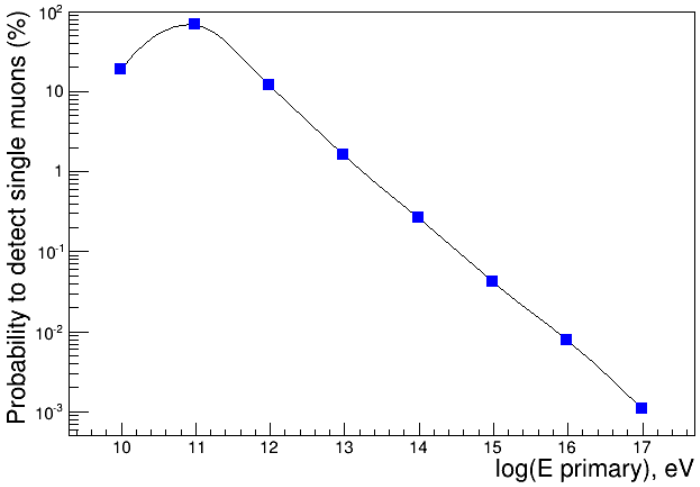

Fig. 3. Probability to detect individual muons as a function of the energy of the primary proton.

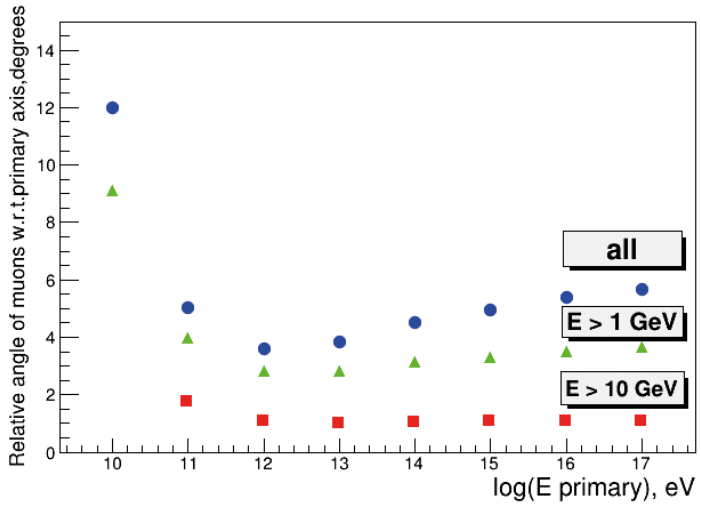

Fig. 4. Average relative angle of secondary muons with respect to primary axis. The blue dots show all muons, while green triangles and red squares report the values obtained for those muons with energy larger than 1 and 10 GeV, respectively.

3.3 Multiple scattering due to the presence of the building

Another factor which in principle may affect the reconstruction of the orientation of a charged particle moving through a dense material is the amount of multiple scattering suffered along its path. Although believed to be of less importance with respect to the previous one, quantitative estimation of this effect was done by means of a GEANT simulation incorporating the possible presence of concrete layers above the EEE telescope in a typical installation. Over the various EEE sites, telescopes are located in very different environments, ranging from a very light roof to several concrete layers, as is the case for instance of those installations where the telescope is located at the ground floor (or even in the underground floor) of a tall building with several floors and solid walls around it. Layers in the building were modelled for simplicity as solid concrete blocks (whose actual composition was introduced in the simulation) with uniform composition, even though the mechanical structure of such layers in reality has a complex shape with empty parts, iron and concrete parts. Taking into account a realistic geometry and the material composition of the layer separating one floor from the other in a modern building, it may be estimated that the overall effect of a single layer on the average energy loss and multiple scattering of muons roughly corresponds to that introduced by 10–15 cm of solid concrete.

The average scattering angle was evaluated in our case as a function of the concrete thickness, and for several values of the muon momentum, from 0.5 GeV/c to 3 GeV/c, since it is well known that this effect is larger for small momentum particles. The results are shown in fig. 5. One can see that the effect of multiple scattering for most of

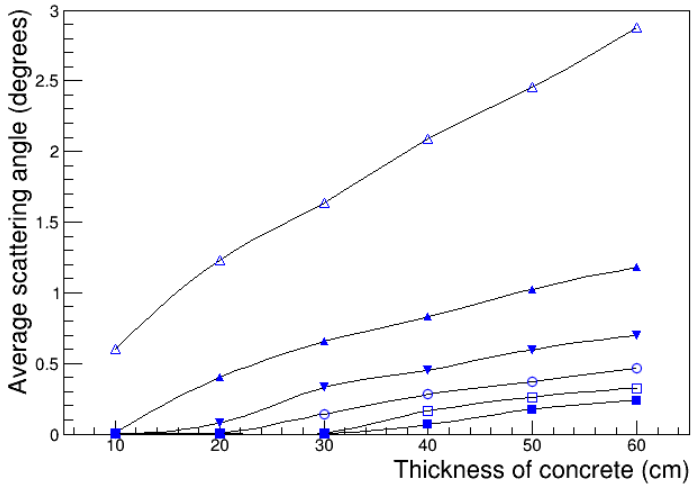

Fig. 5. Scattering angle of secondary muons with respect to their original direction, as a function of the thickness of traversed concrete. From top to bottom, data refer to muons of increasing momentum (0.5, 1.0, 1.5, 2.0, 2.5 and 3.0 GeV/c).

the muons in the range 1–3 GeV/c stays well below 1° even for heavy shielding around the detector, so it is not the dominant term in the uncertainty of the original primary direction.

3.4 Acceptance and time exposure corrections

Due to the rectangular shape of the EEE chambers and their relative distance (which range between 40 cm and 80 cm over the different sites), the geometrical acceptance of a particular telescope is not uniform and must be corrected even to reconstruct the muon angular distributions in local coordinates (ϑ, φ). Moreover, the data taking may be affected by interruptions over long periods, resulting in partial coverage of the sky map in equatorial coordinates during each specific 24 hour period. For these reasons, it is quite mandatory to evaluate the specific acceptance in (Right Ascension, Declination) of each particular telescope, taking into account not only its geometry but also the effective periods of data taking (time exposure).

Detecting a signal anisotropy of the order of 10^{-3} or even smaller with respect to the average isotropic flux of cosmic rays is an experimental challenge, which requires the knowledge of the time exposure and geometrical acceptance of the detector with an accuracy well below the level of expected anisotropy. Since usually this degree of precision cannot be obtained, due to the many factors affecting the stability of a detector over long data taking periods, the commonly adopted solution is to estimate offline the correction, by the use of statistical methods applied to the overall availale dataset. Among the various algorithms devised to estimate the correction factors, those based on the time average of the collected data are the most used [19]. The time average can be conveniently performed by using Monte Carlo techniques through the *scrambling* or *shuffling* procedure. This is a widely used procedure to obtain corrected data from raw data. Basically, it considers two (RA, Dec) maps. The Data map is obtained from real events considering the values (ϑ, φ, t) of the local coordinate angles ϑ, φ, together with associated time t of the event, and transforming these values into (Right Ascension, Declination) variables. A reference map is also obtained by considering the same (ϑ, φ) muon orientation, associated to the time t_R of a random event chosen within a period where the running conditions are believed to be stable. In our case a 24 hours period was assumed, in order to carry out the analysis on a daily basis. A corrected map is then obtained by the ratio between the data map and the reference map. A value of unity in such map means then isotropy. To reduce the statistical error on the reference map, 20 fake events were generated for each real event, with a proper normalization. As an example, fig. 6 shows the raw Data map (top), the reference map (middle) and the corrected map (bottom) for a single day of data taking. Taking into account the considerations of the previous sections, a grid of $3° \times 3°$ was used.

The small dots along the equator in fig. 6 (bottom) are only border effects, since at declinations close to the equator the acceptance of the telescope is very small and the statistics is not adequate. For such reason, the analysis in the following figures was limited to the declination interval (20°, 60°) where the results are more meaningful. The vertical scales of top and middle maps is different by a factor 20 as expected, since the reference map was evaluated considering 20 fake events for each real event.

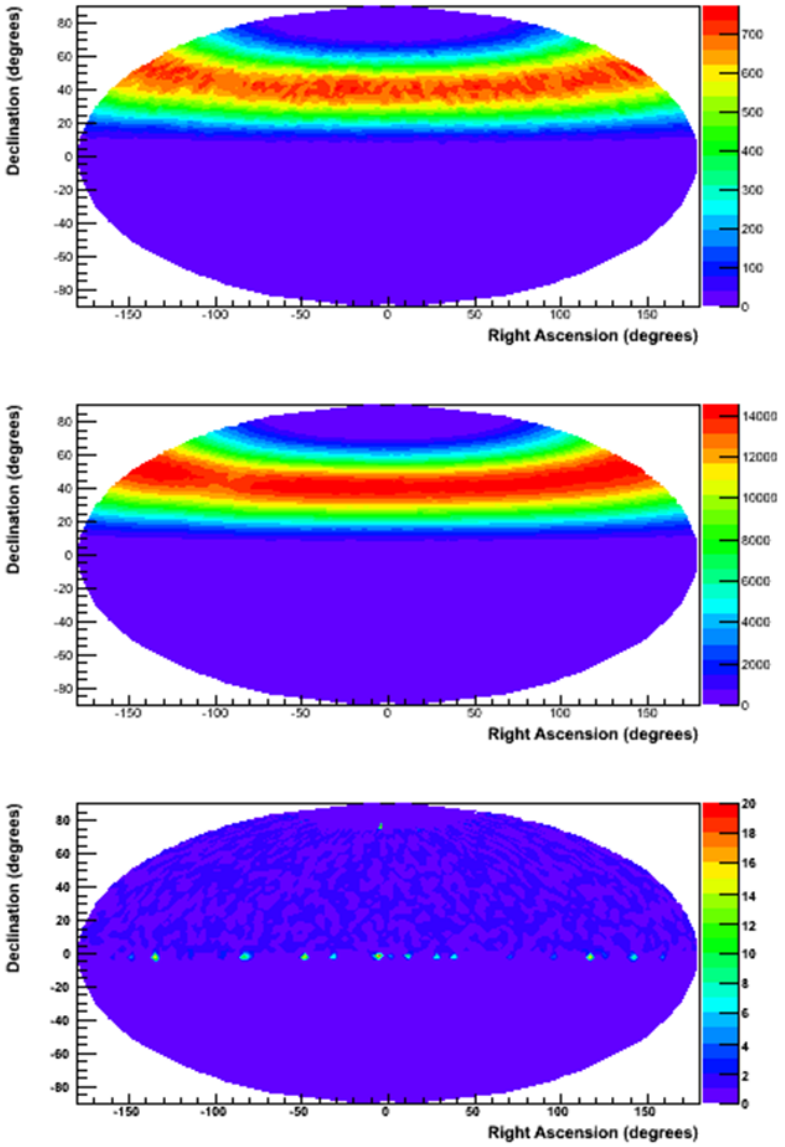

Fig. 6. Aitoff projections of the sky showing raw data (top map) and reference data, generated by the *scrambling* procedure (middle). The normalized ratio between the two maps gives the corrected map, shown on the bottom.

4 Experimental results and discussion

Various datasets, from different telescopes, were analysed in the present paper, to demonstrate the feasibility of the approach for an extended network of detectors, to compare results obtained in different geographical locations and look at the sky map to search for possible deviations from an isotropic pattern. An overall number of about 110 M events was considered in the present analysis, as shown in table 1, which lists the EEE sites, their geographical locations and the number of analysed events.

Results obtained from each day in a single telescope station were summed together, with a weight proportional to the number of collected events in each day. figs. 7–10 show the corrected maps for the four sites. Due to the geometrical acceptance of the telescopes, the range between 20° and 60° was considered, to avoid border effects where statistics is low and correspondingly higher statistical fluctuations are observed. For each individual sky map the average number of events in each grid cell ($3° \times 3°$) is of the order of 10^4, with statistical uncertainties around 1%. Apart from a few cells, mostly located close to the border regions, the majority of the cells exhibit variations within 2–3%, compatible with the isotropy hypothesis, within the statistical uncertainties associated to the number of events analysed. For the data shown in fig. 9, which have the largest statistics, fluctuations are even smaller.

Table 1. Summary of the datasets analysed in the present paper, together with the relevant information from the corresponding EEE site.

EEE Site (Location)	Geographical location	Number of analysed events
SAVO-01 (Savona)	44° 18.366′ N, 8° 28.078′ E	48.6 M
CAGL-01 (Cagliari)	39° 13.767′ N, 9° 7.084′ E	16.6 M
TRIN-01 (Trinitapoli)	41° 21.167′ N, 16° 5.004′ E	20.2 M
CATA-01 (Catania)	37° 31.501′ N, 15° 4.046′ E	19.3 M

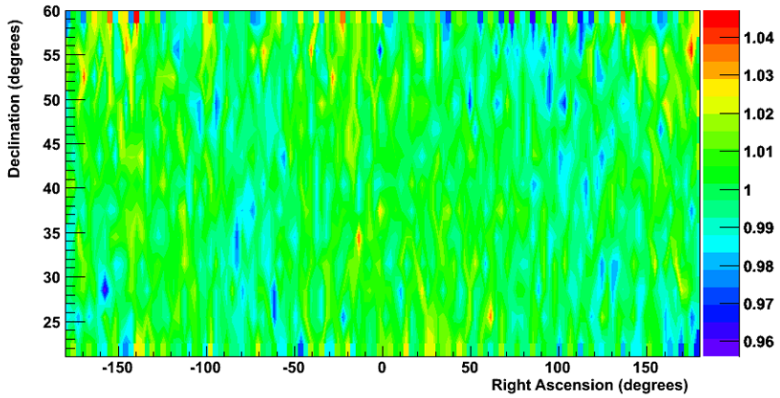

Fig. 7. Equatorial coordinate map for the CAGL-01 site.

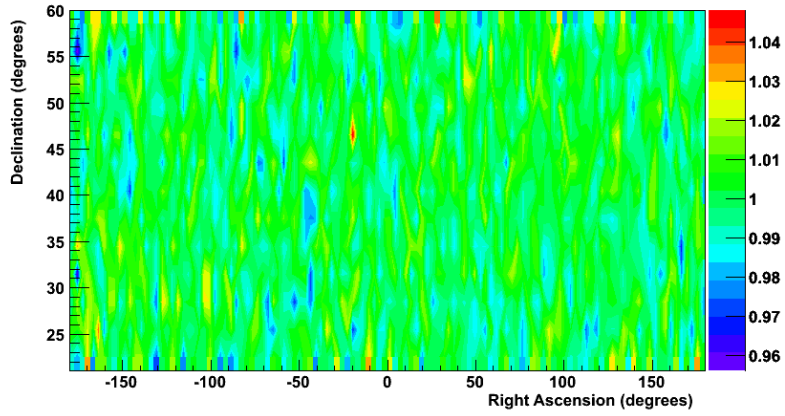

Fig. 8. Equatorial coordinate map for the TRIN-01 site.

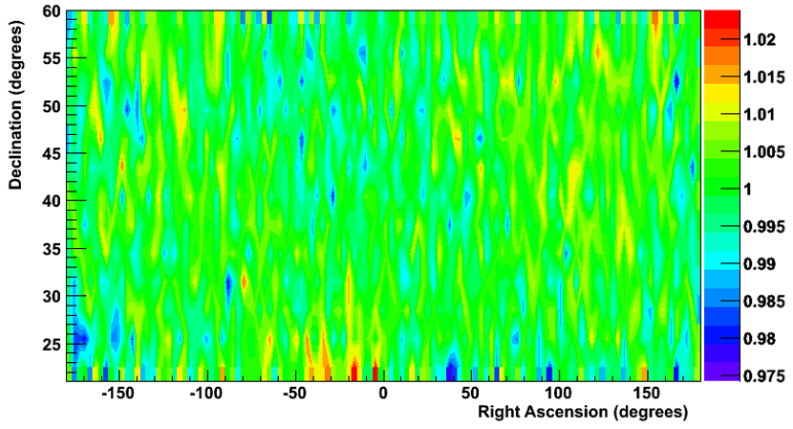

Fig. 9. Equatorial coordinate map for the SAVO-01 site.

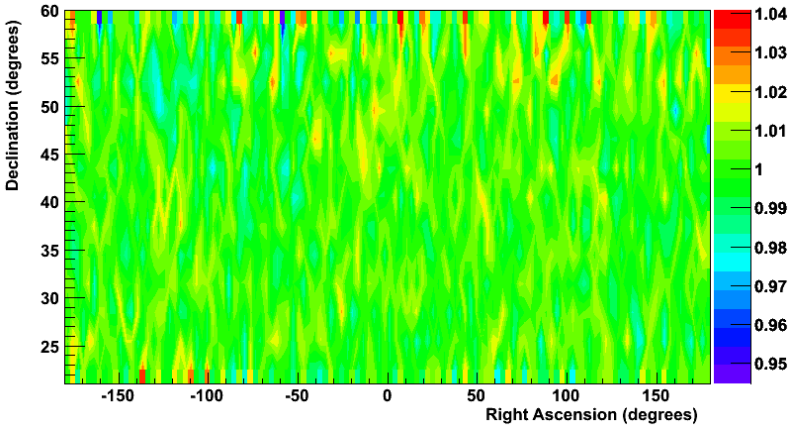

Fig. 10. Equatorial coordinate map for the CATA-01 site.

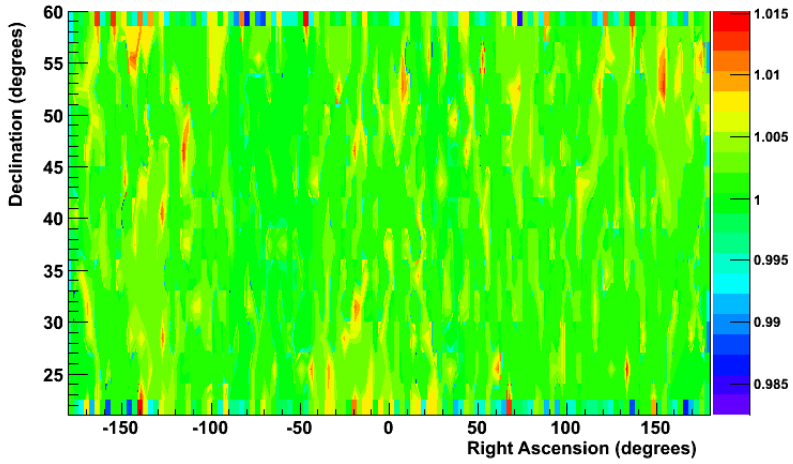

Fig. 11. Equatorial coordinate map summed over the available statistics from the different sites.

Since the geographical locations of the various EEE sites are not too different from each other at sea level, with a similar amount of shielding above them (hence similar muon thresholds), one can sum the various maps with a proper weight given by the number of events collected in each site. The result is reported in fig. 11, which shows how the cell-to-cell fluctuations are further reduced, down to the level of 0.5%.

5 Conclusion

A first analysis of a dataset of cosmic muon tracks detected in various sites of the EEE network has been carried out to build a skymap in equatorial coordinates and look for possible anisotropies in an energy region of the primary cosmics dominated by sub-TeV extensive air showers, where the influence of the eliosphere and local magnetic fields could play an important role. More than 100 M events, collected by four EEE telescopes distributed over the Italian territory, were fully reconstructed after track quality selection. Raw data were corrected for the time exposure of each telescope and its geometrical acceptance by the *scrambling* method, and corrected maps were extracted and plotted as a function of the Right Ascension and Declination, in the Declination range between 20° and 60°. Corrected data maps are compatible with isotropic distributions at the level of 5×10^{-3}–10^{-2}, resulting from the statistical fluctuations associated to the number of analysed events.

The amount of analysed data is currently only a small fraction of the overall statistics collected so far by the EEE network. The recent RUN1, which lasted for two months, gave approximately 4×10^9 events, a factor 40 larger with respect to the sample analysed in the present paper, and the ongoing data taking will give the possibility to increase the available data sample even further, allowing for inhomogeneities down to 10^{-3}. Additional analyses will be carried out in the near future to search for possible deviations from an isotropic pattern at a deeper confidence level.

We are warmly grateful to the many teachers and students of the high schools in Italy involved in the EEE Project, who have made this experiment possible thanks to their enthusiasm and skillful application. We also acknowledge the continuous support of CERN and INFN.

References

1. A.H. Compton, I.A. Getting, Phys. Rev. **47**, 817 (1935).
2. M. Aglietta *et al.*, Astrophys. J. **470**, 501 (1996).
3. M. Amenomori *et al.*, Phys. Rev. Lett. **93**, 61101 (2004).
4. R. Abbasi *et al.*, Astrophys. J. **718**, L194 (2010).
5. G. Guillian *et al.*, Phys. Rev. D **75**, 063002 (2007).
6. M. Amenomori *et al.*, Science **314**, 439 (2006).
7. A.A. Abdo *et al.*, Astrophys. J. **698**, 2121 (2009).
8. K. Nagashima, K. Fujimoto, R.M. Jacklyn, J. Geophys. Res. **103**, 17429 (1998).
9. Centro Fermi Web site: `www.centrofermi.it/EEE`.
10. M. Abbrescia *et al.* (The EEE Collaboration), Nuovo Cimento **125**, 243 (2010).
11. R. Antolini *et al.* (The EEE Collaboration), Nucl. Phys. B **165**, 333 (2007).
12. M. Abbrescia *et al.* (The EEE Collaboration), Nucl. Phys. B **190**, 38 (2009).
13. M. Abbrescia *et al.* (The EEE Collaboration), Eur. Phys. J. Plus **127**, 42 (2012).
14. M. Abbrescia *et al.* (The EEE Collaboration), Nucl. Instrum. Methods Phys. Res. A **588**, 211 (2008).
15. M. Abbrescia *et al.* (The EEE Collaboration), Nucl. Instrum. Methods Phys. Res. A **593**, 263 (2008).
16. M. Abbrescia *et al.* (The EEE Collaboration), Eur. Phys. J. Plus **128**, 62 (2013).
17. P. Duffet-Smith, J. Swart, *Practical Astronomy with your calculator or spreadsheet* (Cambridge University Press 2011).
18. D. Heck *et al.*, Report FZKA 6019 (1998), Forschungszentrum 618 Karlsruhe.
19. R. Iuppa, G. Di Sciascio, Astrophys. J. **766**, 96 (2013).